Characteristics of ground-level enhancement–associated solar flares, coronal mass ejections, and solar energetic particles

K. A. Firoz,[1] K.-S. Cho,[1] J. Hwang,[1] D. V. Phani Kumar,[1] J. J. Lee,[1] S. Y. Oh,[2] Subhash C. Kaushik,[3] Karel Kudela,[4] Milan Rybanský,[4] and Lev I. Dorman[5,6]

Received 26 October 2009; revised 5 April 2010; accepted 16 April 2010; published 14 September 2010.

[1] Ground-level enhancements (GLEs) are sudden, sharp, and short-lived increases in cosmic ray intensities registered by neutron monitors. These enhancements are known to take place during powerful solar eruptions. In the present investigation, the cosmic ray intensities registered by the Oulu neutron monitor have been studied for the period between January 1979 and July 2009. Over this span of time, increase rates of 32 GLEs have been deduced. In addition, we have studied characteristics of the 32 event-associated solar flares, coronal mass ejections (CMEs), and solar energetic particle (SEP) fluxes. We found that all of the 32 GLEs were associated with solar flares, CMEs, and SEP fluxes. Approximately 82% of the events were associated with X-class flares. Most of the flares that were associated with GLEs of increase rates >10% originated from the active regions located on the southwest hemisphere of the Sun. The average speed (1726.17 km/s) of GLE-associated CMEs was much faster than the average speed (423.39 km/s) of non-GLE-associated CMEs. It also became evident that ~67% GLEs were associated with very fast (>1500 km/s) CMEs. Although a GLE event is often associated with a fast CME, this alone does not necessarily cause the enhancement. Solar flares with strong optical signatures may sometimes cause GLE. High SEP fluxes often seem to be responsible for causing GLEs as the correlation with SEP fluxes implies.

Citation: Firoz, K. A., K.-S. Cho, J. Hwang, D. V. Phani Kumar, J. J. Lee, S. Y. Oh, S. C. Kaushik, K. Kudela, M. Rybanský, and L. I. Dorman (2010), Characteristics of ground-level enhancement–associated solar flares, coronal mass ejections, and solar energetic particles, *J. Geophys. Res.*, *115*, A09105, doi:10.1029/2009JA015023.

1. Introduction

[2] Cosmic rays are high-energy particles. They originate from different sources such as remnants of supernovae, neutron stars, black holes, objects in radio galaxies, and sometimes events in our Sun and its heliosphere [e.g., *Hillas*, 1972; *Gaisser*, 1990; *Longair*, 1992; *Firoz et al.*, 2009]. They undergo collisions with atoms of the upper atmosphere and produce a cascade of secondary particles that shower down onto the surface of the Earth. Ground level enhancements (GLEs) are increases of cosmic ray intensity measured on the Earth's ground. Solar energetic particles (SEPs), solar flares, and/or coronal mass ejections (CMEs) are also normally observed when GLEs occur, suggesting that these are causing GLEs or are caused by the same process in the Sun or its corona.

[3] SEPs, solar flares, and CMEs are produced in sporadic solar eruptions. Solar flares and CMEs are in the larger ones. The distinction between solar flare and CME is that a solar flare is a sudden flash of electromagnetic radiation, whereas a CME is a mass motion in the solar corona that can be seen in a coronagraph. The spatial relation between flares and CMEs depends on the magnetic field configurations involved in the solar eruption process. Flares are perhaps photospheric and CMEs are chromospheric. The flares erupt from the intensely luminous area of the Sun, whereas the CMEs are ejected from an incandescent and transparent layer of gas lying above and surrounding the photosphere. So flares can presumably trigger CMEs. However, there are also arguments that both phenomena might originate from the same active region of the solar disk even though they have different manifestations. Detailed explanations can be found in several studies [e.g., *Kahler et al.*, 1978; *Cliver et al.*, 1982; *Harrison*, 1995; *Kahler et al.*, 2001; *Dorman*, 2004; *Kurt et al.*, 2004; *Jing et al.*, 2005; *Yashiro et al.*, 2008; *Belov*, 2009].

[4] The solar energetic particles having intense fluxes in near Earth space are of great interest, in particular, because

[1]Solar and Space Weather Research Group, Korea Astronomy and Space Science Institute, Daejeon, South Korea.
[2]Bartol Research Institute, University of Delaware, Newark, Delaware, USA.
[3]School of Studies in Physics, Jiwaji University, Gwalior, India.
[4]Institute of Experimental Physics, Slovak Academy of Sciences, Košice, Slovakia.
[5]Israel Cosmic Ray and Space Weather Center and Emilio Segre' Observatory, Technion and Israel Space Agency, Qazrin, Israel.
[6]Also at Cosmic Ray Department, N.V. Pushkov IZMIRAN, Russian Academy of Sciences, Moscow, Russia.

Copyright 2010 by the American Geophysical Union.
0148-0227/10/2009JA015023

of their impacts on cosmic ray modulation. Those particles spread near the Sun and are carried away by CME-driven shock waves propagating through the interplanetary space. The propagation process may accelerate particles to higher energies that intensify the cosmic ray intensity to a sharp increase. Once the acceleration of particles ends, the sharp rise of cosmic ray intensity measured at the ground with neutron monitors returns to the background level or close to the background level within tens of minutes to hours. Flare and CME-driven shock reconnection may also cause a sharp rise in the cosmic ray intensity at the Earth. If the particles accelerate to sufficiently high energies (gigaelectron volts) and the intensity is sufficiently high, then enhancements at the ground (GLEs) are also thought to occur. Registration of GLE events by ground-based neutron monitors began in the early 1940s. More details can be studied in a number of papers and books [e.g., *Meyer et al.*, 1956; *Park*, 1957; *Dorman and Venkatesan*, 1993; *Kudela et al.*, 1993; *Reames*, 1995; *Shea et al.*, 1999; *Miroshnichenko*, 2001; *Duldig*, 2001; *Smart and Shea*, 2002; *Cliver et al.*, 2004; *Gopalswamy et al.*, 2005].

[5] SEP fluxes at different energy channels can be weighed by their corresponding fluences, which are typically measured by satellites in geostationary orbits. They demonstrate a different asymmetry relative to minimum and maximum states of solar activity cycle. SEP fluxes are observed with energy of megaelectron volts, whereas GLEs are thought to require a typical energy of gigaelectron volts to be high enough for the particles to penetrate the Earth's atmosphere. [e.g., *Dorman and Venkatesan*, 1993; *Cliver et al.*, 2004; *Cliver*, 2006; *Dorman and Pustil'nik*, 2005; *Belov et al.*, 2005; *Flückiger et al.*, 2006; *Mavromichalaki et al.*, 2007].

[6] Intense solar flares and fast CMEs consisting of entrained magnetic fields have enough potential to create turmoil in the Earth's atmosphere [e.g., *Manchester et al.*, 2005; *Wang and Wang*, 2006]. Namely, electromagnetic emissions produced by solar flares penetrate the Earth's atmosphere and change particle environment on the Earth, consequently disrupting radio transmissions. SEPs that are accelerated at solar eruptive event can propagate to the Earth, causing damage to satellite electronics and posing radiation hazards to astronauts and aircrews [*Braun et al.*, 2005; *Firoz and Kudela*, 2007]. Thus, SEP fluxes, X-ray flares, and CMEs may also cause sharp rises in cosmic ray intensities in the Earth. So, a study on characteristics of GLE-associated SEPs, X-ray flares, and CMEs can be useful for the understanding of cosmic rays and space weather. This is our motivation to pursue this study.

[7] To our knowledge, a method demonstrating how to estimate an increase rate (%) of the cosmic ray intensity (CRI) of GLE events has not yet been shown. Furthermore, characteristics of GLE-associated solar flares, CMEs, and SEP fluxes including solar cycle 23 have been studied only in part at the present time. Hence, we will show how to deduce the increase rate (%) of the CRI of GLE events, thereby presenting a catalog of increase rate, its start time, peak time, and the time difference with associated solar agents, such as X-ray solar flare, CME, etc. Then, we will explain the characteristics of GLE-associated X-ray flares, CMEs, and SEPs, subsequently searching for the perpetrators that seem to be responsible for causing GLEs.

2. Data Deductions and Analyses

2.1. Cosmic Ray Intensity

[8] We analyzed the data of CRI registered by Oulu neutron monitor (see http://cosmicrays.oulu.fi/) for the period of January 1979 through July 2009. The Oulu neutron monitor (ONM) station is situated at the height of 15 m above sea level in the geographic coordinates of latitude 65.05°N and longitude 25.47°E. It is a standard 9-NM-64 consisting of three units with each of three counters. We preferred CRI data from the ONM station for this study because it has high-resolution data for a long time period. The lists of GLEs given in the catalog of the ONM have been considered as references. According to the occurrence time of GLEs, we analyzed 5 min data of CRI. Based on the availability of 5 min pressure corrected data, we deduced increase rates (%) of 32 GLE events for this study. The method for deducing the increase rate of GLE that we used is given as follows.

[9] The preincrease of the CRI of GLE is the background count rate preceding the time CRI starts increasing toward a sharp rise. To measure the increment of the sharp rise, the average of the preincrease is considered as the common background. The difference between each 5 min CRI and the average of the preincrease is the increment above the common background level. The increase rate (%) of the CRI of GLE is computed by the following expression:

$$I_r(\%) = \left[\left\{\left(I_j - I_{pv}\right) \times 100\right\}/I_{pv}\right], \quad (1)$$

where I_r (%) is the increase rate of CRI, I_j is the CRI of the time series from the preincrease value to the value at which the CRI decreases to minimum or to the background level, I_{pv} is the average CRI of preincrease before the onset of the sharp increase. In equation (1), subscript r denotes rate and j stands for the CRI of the time window of each GLE event. The time window of each GLE event is considered within 24 hours, covering backgrounds before and after the GLE peaks. Therefore, the time window of each GLE event has 288 number of CRI (j = 1, 2, …, 288) based on 5 min data. The subscript pv stands for the average of preincrease. This deduction process also satisfies the criteria mentioned in the catalog of the ONM (see http://cosmicrays.oulu.fi/).

[10] The peak time (T_{pkc}) of the GLE is where the highest peak intensity (I_{pkc}) of the sharp rise of the CRI is observed. On the other hand, the start time of the GLE is where the increase rate (%) is found above "zero" level within any time right before the peak time of GLE. The duration of GLE is the length of time between the moment the increase rate (%) starts rising up above zero level and the moment it minimizes again to zero level. As an example, Figure 1 clarifies how the peak time (T_{pkc}), start time (T_{stc}), and end time (T_{end}) of the GLE have been deduced. If the GLE was seen at the very end of the day, we investigated, in addition, the day immediately following to check the end time of the GLE. If the GLE was seen at the very beginning of the day, we also investigated the day immediately pre-

21562202a, 2010, A9, Downloaded from https://agupubs.onlinelibrary.wiley.com/doi/10.1029/2009JA015023, Wiley Online Library on [13/06/2025]. See the Terms and Conditions (https://onlinelibrary.wiley.com/terms-and-conditions) on Wiley Online Library for rules of use; OA articles are governed by the applicable Creative Commons License

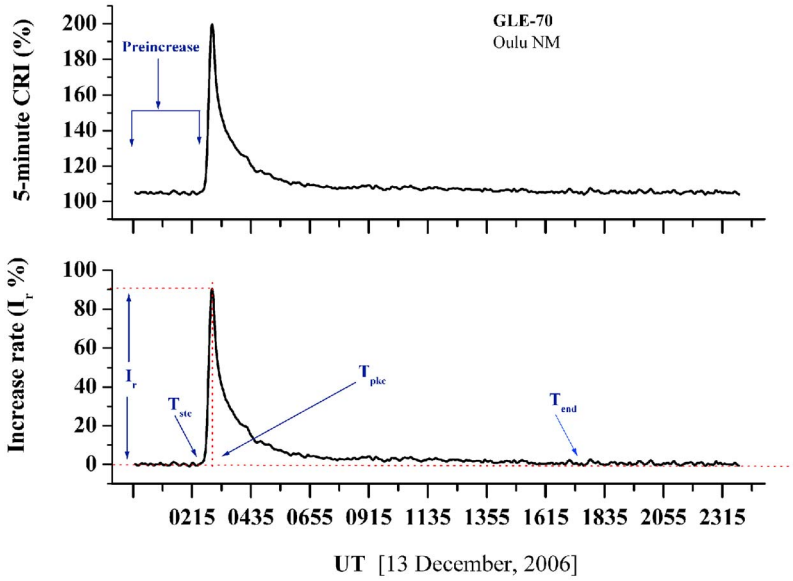

Figure 1. An example of how to deduce the increase rate (%) of GLE is shown. (top) The 5 min CRI at ONM for GLE70 occurred on December 13, 2006 and (bottom) its increase rate (%) is shown. The peak time (T_{pkc}) of the GLE is when the increase rate (I_r) (%) is the highest. The start time (T_{stc}) is when the I_r (%) starts increasing above zero level, and the end time (T_{end}) is when it minimizes again to zero level. GLE, ground-level enhancements; CRI, cosmic ray intensity; ONM, Oulu Neutron Monitor.

ceding to search the start time and the preincrease count rate. Thus, we investigated the 5 min data for 24 hours of each GLE event. Based on the availability of 5 min simultaneous data of CRI, by utilizing equation (1) and its procedure explained above, we deduced the start time (T_{stc}), peak time (T_{pkc}), and increase rate (I_r %) of 32 GLE events at ONM. These are noted in Table 2.

[11] We found a few GLE events in which increase rates (I_r %) are very high. So, we further analyzed hourly data of CRI for confirmation. To evaluate the consistency of the data, we checked the amplitude, phase, and dispersion of the daily averaged CRI by means of the least squares method used earlier by a few authors [*Firoz and Kudela*, 2007; *Firoz*, 2008; *Firoz et al.*, 2009]. As a result, there was clearer

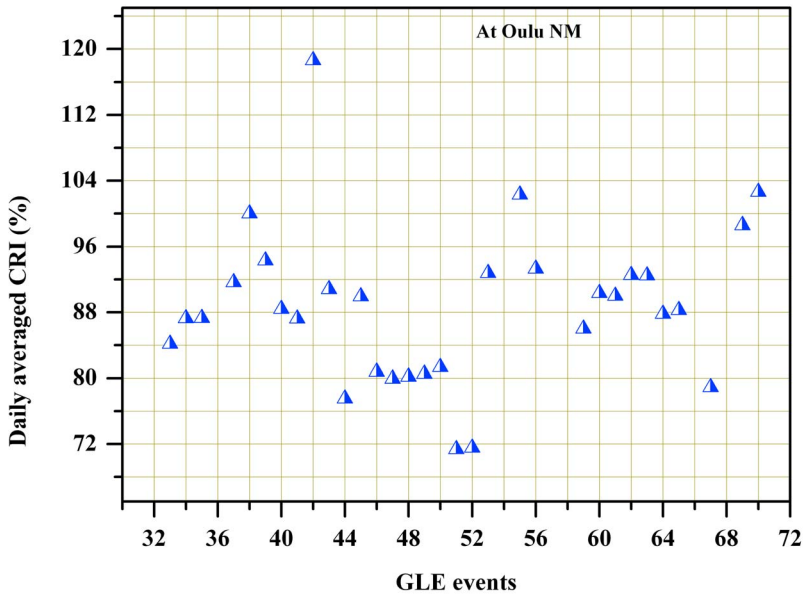

Figure 2. Daily averaged cosmic ray intensity (CRI) (%) at Oulu neutron monitor (ONM) for the 32 GLE events given in Table 2 is exhibited. The daily averaged 32 GLE events follow the general trend of inverse proportionality with the solar activity cycle.

21562202a, 2010, A9, Downloaded from https://agupubs.onlinelibrary.wiley.com/doi/10.1029/2009JA015023, Wiley Online Library on [13/06/2025]. See the Terms and Conditions (https://onlinelibrary.wiley.com/terms-and-conditions) on Wiley Online Library for rules of use; OA articles are governed by the applicable Creative Commons License

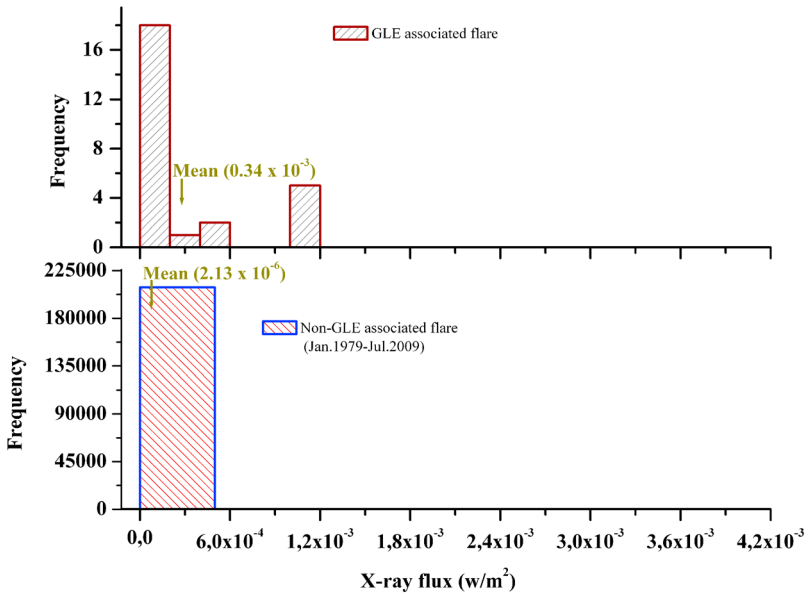

Figure 3. (top) The distributions of X-ray fluxes associated with 32 GLEs. (bottom) The distributions of non-GLE associated X-ray fluxes. The criteria of classification explained in flare analysis (section 2.2) have been obeyed throughout. GLE, ground-level enhancements.

understanding of the statuses of the selected 32 GLEs (Figure 2). Figure 2 indicates that the daily averaged CRIs of GLE events also obey the general trends of periodicity of diurnal cosmic ray cycles.

2.2. X-Ray Fluxes, CMEs, and SEPs

[12] Data of the intensity-time profiles of X-ray fluxes and SEP fluxes of several energy bands have been downloaded from Geostationary Operational Environmental Satellite (GOES) (see http://goes.ngdc.noaa.gov/). Data of SEP fluences of available energy bands have been collected from the National Geophysical Data Center (NGDC) (see http://www.ngdc.noaa.gov/stp/SOLAR/ftpsatenvir.html). SEP events sometimes correspond to GLE events, and hence SEP events of energy channel >10 MeV available in the catalog of the National Oceanic and Atmospheric Administration (NOAA) (see http://umbra.nascom.nasa.gov/SEP/) have also been checked.

[13] Data of CMEs observed by Large Angle Spectrometric Coronagraph (LASCO) C2 and C3 onboard Solar and Heliospheric Observatory (SOHO) since 1996 have been studied in the catalog of the Coordinated Data Analysis Workshop (CDAW) (see http://cdaw.gsfc.nasa.gov/CME_list/). We considered the first appearance time (T_{cme}) of CME in the LASCO C2 field of view, sky plane linear speed (V_{cme}), central position angle (CPA), and angular width (AW) of the CMEs. Halo and non-Halo CMEs have also been studied to understand the difference. The Halo CME is inherently wider and has more potential than the non-Halo CME. Observer's position determines Halo or non-Halo CME.

[14] The 5 min data of X-ray fluxes and SEP fluxes recorded by different satellites of GOES have been utilized. The GOES satellite whose data has mostly been used for this study is GOES-6. Sometimes, we also used the data of the GOES-8 and GOES-10 satellites in case of any unavailability of the data from GOES-6. Classes of X-ray solar flares are categorized according to the order of the magnitude of the peak burst intensity measured at the Earth by the satellites within the wavelength band between 0.1 and 0.8 nm. The classifications of flares are accomplished by the criteria defined in the NGDC catalog.

3. Observations

3.1. Characteristics of GLE-Associated Solar Flare

[15] Solar flare is usually produced in large solar eruptions. It is spewed out as a sudden flash of electromagnetic radiation emission from the active region of the intensely luminous part of the Sun. The intense or harder electromagnetic radiation emissions refer to the intense or harder portion of X-ray fluxes [*Meyer et al.*, 1956; *Dennis and Zarro*, 1993]. So, the weak and intense portions of X-ray fluxes can be investigated with the simultaneous CRI of each GLE event to understand the quantitative association between solar flare and GLE event.

[16] In this context, we investigated GLE and non-GLE-associated solar flare events. We found that most of the GLEs were associated with strong flares. In most cases, an X-class (0.34×10^{-3} w/m^2) solar flare occurred just before GLE events, whereas most C-class (2.13×10^{-6} w/m^2) flares without GLE events were taken place (Figure 3). There are several cases where M-class flares or even C-class flares with optical importance >1N were also found associated with GLE events. That means, regardless of class, a flare with high optical brightness may also be strong enough to cause a GLE event. According to the observations noted in Table 1, almost 82% (26/32) of the GLE-associated flares were X-class flares, whereas 6% (2/32) were M-class flares, and 12% (4/32) were C-class flares. Ninety-four percent of flares had optical importance within the range of 1N to 4B.

21562202a, 2010, A9, Downloaded from https://agupubs.onlinelibrary.wiley.com/doi/10.1029/2009JA015023, Wiley Online Library on [13/06/2025]. See the Terms and Conditions (https://onlinelibrary.wiley.com/terms-and-conditions) on Wiley Online Library for rules of use; OA articles are governed by the applicable Creative Commons License

Table 1. GLE Events[a]

GLE Event[b]		X-ray Flux (w/m^2)[c]						CME[d]				SEP Event[e]			Type II Radio Burst[g]	
No.	Date (DD.MM.YY)	T_{stf}(UT)	T_{pkf}(UT)	T_{endf}(UT)	Class	Opt. Imp.	AR	T_{ap}(UT)	V_{cme}(km/s)	CPA (deg)	AW (deg)	PF > 10 MeV	T_{st}(UT)	Fluence PF > 10 MeV (per cm^2) [f]	T_{str}(UT)	T_{endr}(UT)
33	21.08.79	0611	0613	0645	C6.0	1B	N15W38					500	0740		0607	0645
34	10.04.81	1632	1703	1704	X2.5	3B	N07W35					50	1745		1644	1650
35	10.05.81	0712	0731	0751	M13	–	–					150	2130		0603	0743
37	26.11.82	0230	0237	0320	X4.5	2B	S11W87					25	0605		0226	0235
38	07.12.82	2336	2354	2447	X2.8	–	–					–	–		2340	0000
39	16.02.84	0736	0743	0753	C2.3	–	–					660	0915		0858	0900
40	25.07.89	0839	0843	0908	X2.6	2N	N25W84					54	1225	1.6e6	0844	0905
41	16.08.89	0108	0117	0228	X20.0	2N	S18W84					–	–	1.2e8	0103	0129
42	29.09.89	1047	1133	1435	X9.8	–	S26W90					4500	1205	1.0e8	1122	1141
43	19.10.89	1229	1255	2013	X13.0	4B	S27E10					40000	1305	5.4e7	1250	1313
44	22.10.89	1708	1757	2108	X2.9	2B	S27W31					–	–	–	1742	1743
45	24.10.89	1736	1831	2624	X5.7	3B	S30W57					–	–	1.4e8	1740	1744
46	15.11.89	0638	0705	0920	X3.2	3B	N11W26					71	0735	1.4e6	0655	0658
47	21.05.90	2212	2217	2339	X5.5	2B	N35W36					410	2355	8.1e4	2212	2240
48	24.05.90	2046	2049	2145	X9.3	1B	N33W78					180	2125	8.2e5	2048	2100
49	26.05.90	2045	2058	2133	X1.4	–	–					–	–	4.0e6	2048	2114
50	28.05.90	0723	0808	0831	C3.0	F	S15W44					45	0715	1.8e6	0838	0839
51	11.06.91	0209	0229	0320	X12.0	3B	N31W17					3000	1420	7.9e7	0202	0335
52	15.06.91	0633	0831	1117	X12.0	3B	N33W69					1400	1950	4.1e7	0645	0646
53	25.06.92	1947	2011	2229	X3.9	2B	N09W67					390	0610	7.1e5	1954	1956
55	06.11.97	1149	1155	1201	X9.4	2B	S18W63	1210	1556	Halo	360	490	1305	8.5e6	1152	1217
56	02.05.98	1331	1342	1351	X1.1	3B	S15W15	1406	938	Halo	360	150	1420	2.4e6	1338	1723
59	14.07.00	1003	1024	1043	X5.7	3B	N22W07	1054	1674	Halo	360	24000	1045	2.3e8	1007	1135
60	15.04.01	1319	1350	1355	X14.4	2B	S20W85	1406	1199	245	167	951	1410	2.1e7	1332	1615
61	18.04.01	0211	0214	0216	C2.2	2B	S 20, W limb	0230	2465	Halo	360	321	0315	1.2e7	0217	0233
62	04.11.01	1603	1620	1657	X1.0	3B	N06W18	1635	1810	Halo	360	31700	1705	2.0e7	1611	1715
63	26.12.01	0432	0540	0647	M7.1	1B	N08W54	530	1446	281	>212	779	0605	2.1e6	0501	0810
64	24.08.02	0049	0112	0131	X3.1	1F	S02W81	0127	1913	Halo	360	317	0140	1.7e7	0108	0135
65	28.10.03	0951	1110	1124	X17.2	4B	S16E08	1130	2459	Halo	360	29500	1215	1.8e8	1005	1236
67	02.11.03	1703	1725	1739	X8.3	2B	S14W56	1730	2598	Halo	360	1570	1105	1.5e7	1714	1824
69	20.01.05	0636	0700	0726	X7.1	3B	N14W61	0654	882	Halo	360	-	-	5.2e7	0439	0943
70	13.12.06	0214	0240	0257	X3.4	3B	S06W23	0254	1774	Halo	360	698	0925	2.7e7	0225	0441

[a]N, north latitude of correlated optical flare; S, south latitude of correlated optical flare; E, east central meridian distance of correlated optical flare; W, west central meridian distance of correlated optical flare; Opt. Imp., the optical importance on flare area is categorized as B = bright, N = normal, F = faint.

[b]GLE event number (No.) and its occurrence date.

[c]Start time (T_{stf}), peak time (T_{pkf}), end time (T_{endf}), class, optical importance of X-ray flux, and the active region (AR) of the Sun from which the flare is believed to have been originated.

[d]Time of CME first appearance (T_{ap}) in the LASCO-C2 field of view, linear speed in the sky plane (V_{cme}), central position angle (CPA), and angular width (AW) of the CME.

[e]Solar energetic particle (SEP) event and its start time.

[f]The fluence of SEP.

[g]Solar radio type II burst: start time (T_{str}) and end time (T_{endr}). Over the time window of each GLE, the difference between start and end time of the type II burst has been considered as the duration of shock wave.

215622024, 2010, A9, Downloaded from https://agupubs.onlinelibrary.wiley.com/doi/10.1029/2009JA015023, Wiley Online Library on [13/06/2025]. See the Terms and Conditions (https://onlinelibrary.wiley.com/terms-and-conditions) on Wiley Online Library for rules of use; OA articles are governed by the applicable Creative Commons License

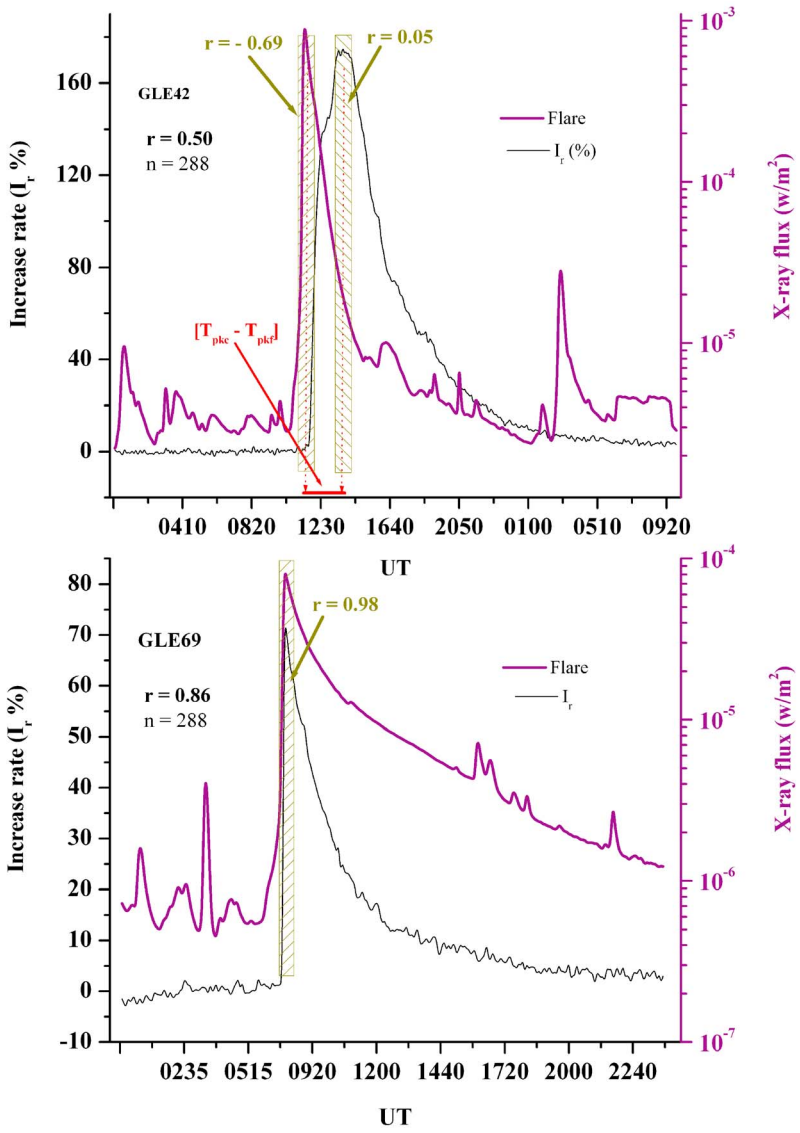

Figure 4. Often flare peaks are little earlier than GLE peaks. At times, peaks of GLE and peaks of flare coincide or more closely time integrated. Here, two examples are shown. (top) Correlation coefficients of GLE peaks with simultaneous X-ray flare peaks are not well correlated, while flare peaks and simultaneous GLE peaks are negatively correlated. This type of GLE is perhaps not produced by solar flares alone. Contrarily, (bottom) GLE peaks coincident with flare peaks or more closely time integrated are positively well correlated. This type of GLE is thought to be produced by solar flares. In Figure 4 (top), comparison between the peak times of X-ray flux (w/m^2) and peak time of increase rate (I_r %) of GLE42 is also shown. The difference between GLE peak time (T_{pkc}) and flare peak time (T_{pkf}) is marked by [$T_{pkc} - T_{pkf}$]. GLE, ground-level enhancements.

This finding is consistent, in general, with *Kudela et al.* [1993], who investigated 38 GLE events (1964–1991) associated with solar flares having optical importance of 1N to 3B. The flares whose classes are C or M having less optical importance than 1N did not seem to cause GLE. However, we found that, for example, the GLE50-associated C-class (C3.0) flares had very low optical importance (1F). Thus, the GLE50 was perhaps not generated by a solar flare.

[17] Solar flares are known to erupt from the active regions of the Sun where the Sun's magnetic field is especially strong. It is found that 54% (22/28) GLE-associated flares originated from the southwest active region, whereas 46% (13/28) GLE-associated solar flares originated from the north-west active region. Most of the X-ray flares that were associated with GLE of increase rate >10% originated from the southwest active region of the Sun. Almost 97% GLE-associated X-ray flares originated from the Western Hemisphere (Table 1), which means that the greater possibility for a GLE is connected with the western X-class flares [e.g., *Duldig*, 1994].

[18] Association of strong flares with a GLE event does not imply precisely that GLE can be produced by solar

21562202a, 2010, A9, Downloaded from https://agupubs.onlinelibrary.wiley.com/doi/10.1029/2009JA015023, Wiley Online Library on [13/06/2025]. See the Terms and Conditions (https://onlinelibrary.wiley.com/terms-and-conditions) on Wiley Online Library for rules of use; OA articles are governed by the applicable Creative Commons License

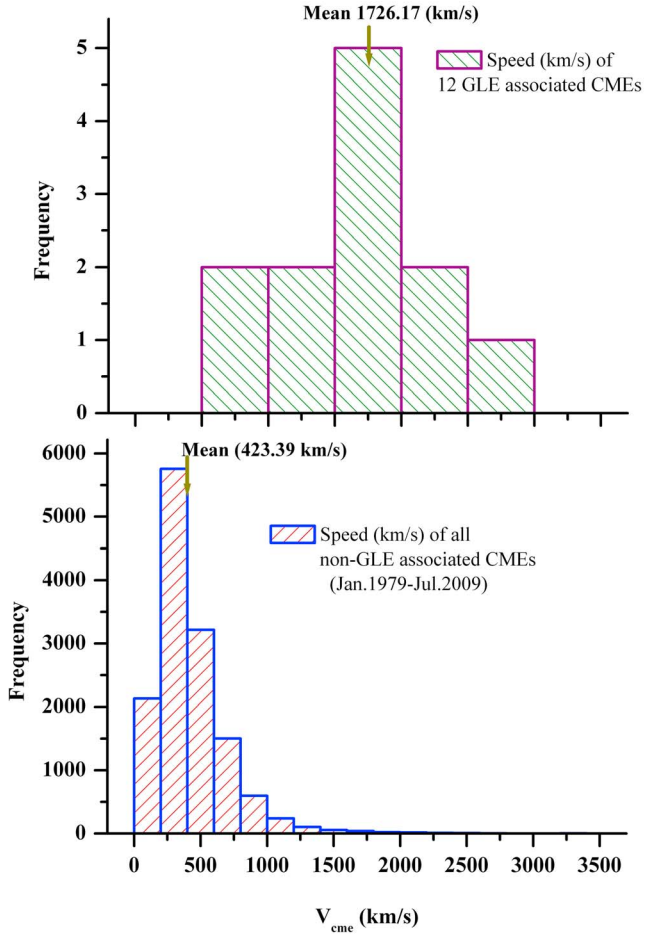

Figure 5. (top) The distributions of the speeds of CMEs associated with GLE events. (bottom) The distributions of the speeds of CMEs associated with non-GLE events. CME, coronal mass ejection; GLE, ground-level enhancements.

flares. The GLE peak is indeed the enhancement that must be checked with simultaneous X-ray flux. The time-integrated rising portion of the flare might be the concern to GLE peak (e.g., Figures 4 and 6). As found, the rising portions of X-ray fluxes are often earlier than the peak time of the GLE and, at times, occur simultaneously. The mean time difference between X-ray solar flare peak and GLE peak is ~75.24 min. Since peaks of solar flares are often earlier than GLE peaks, it was necessary to examine correlation coefficients between GLE peaks and simultaneous X-ray fluxes, and between peaks of X-ray fluxes and simultaneous GLE peaks. Results suggest that some of the GLE peaks seem to be caused by X-ray fluxes, but many are not. It is evident that many of the GLE peaks do not have significant positive correlations with simultaneous X-ray fluxes. We believe that GLEs nearly coincident with X-ray flux peaks are caused by the flare, but presumably another process must be involved when there is a significant delay between the peak in X-ray flux and GLE.

3.2. Characteristics of GLE-Associated CME

[19] Coronal mass ejection is the ejection of magnetized plasmas from the Sun into the solar corona and solar wind [*Shanmugaraju et al.*, 2008]. When the ejected plasma reaches the Earth, it may have an impact on the modulation of cosmic ray intensity. In this context, we investigated GLE and non-GLE-associated CMEs. On an average, the speed (1726.17 km/s) of GLE-associated CMEs is much faster than the speed (423.39 km/s) of non-GLE-associated CMEs (Figure 5). Almost 67% (8/12) GLEs were associated with very fast (>1500 km/s) CMEs in the sky plane.

[20] Although the GLE is usually associated with the fast CMEs, other properties of CMEs should also be considered because the efficiency of the ejection of plasma on the modulation of cosmic rays does not depend only on its speed, but also on its position angle [e.g., *Smart et al.*, 2006]. Halo CME is known to propagate toward the Earth; hence it can modulate cosmic ray intensity at the Earth. From this point of view, it is found that ~84% (10/12) GLEs were associated with Halo CMEs, whereas ~16% (2/12) GLEs were associated with partial Halo CMEs having angular width >166° (Tables 1 and 2). Since GLE is often associated with Halo CMEs, geomagnetic disturbances can be general phenomena in the magnetosphere during GLE occurrence. Geomagnetic disturbances in the Earth's magnetosphere can cause cosmic ray modulation either directly or even inversely depending on the magnitude of the compression caused by CME and other geomagnetic agents.

[21] Results suggest that most of the GLE-associated CMEs had very fast speeds, whereas a few of them were of extremely fast. But it is not clear that CMEs alone can produce GLEs because the CME first appears a few minutes later than the GLE peak. If the CME is triggered from the solar flare, the appearance of CMEs later than the flare can be reasonable. So, the flare may be responsible, but not CME, for causing the GLE event. The difference between CME first appearance time and GLE peak time varied mostly within ~25 min. The time difference did not show that the faster the CME, the more the delay or vice versa. Other CME properties with respect to the time delay also did not indicate any dependence. It further indicates that CME perhaps does not produce the GLE peak.

[22] We understand that the fast CME has the potential to accelerate the interplanetary shock waves during their propagations through the interplanetary medium. CMEs eventually drive shock waves ahead as they propagate, and the acceleration in large SEP fluxes starts at the arrival of the CME-driven shock wave (e.g., Figure 6). The acceleration of particles is believed to take place by the shock. The propagation of the shock is perhaps controlled by the ambient solar wind plasma and aerodynamic drag force. Although shock acceleration occurs widely at sites throughout the heliosphere, the process may have an impact on SEP fluxes near the Earth's space [e.g., *Reames*, 1997; *El-Borie*, 2003; *Vršnak et al.*, 2004]. The conjunction between flares having strong optical signatures and fast CME-driven shocks seems to produce GLEs. Most of the shocks occurred several minutes before the start time of GLEs (Tables 1 and 2). The mean difference between the start time of shocks and the start time of GLEs was ~30 min. This finding supports *Gopalswamy et al.* [2005], who suggested that flare and shock reconnection may contribute to GLE.

[23] *Andrews* [2003] suggested that the strong flares are very likely to be associated with fast CMEs. We confirm that most of the GLEs associated with strong flares are also

21562202a, 2010, A9, Downloaded from https://agupubs.onlinelibrary.wiley.com/doi/10.1029/2009JA015023, Wiley Online Library on [13/06/2025]. See the Terms and Conditions (https://onlinelibrary.wiley.com/terms-and-conditions) on Wiley Online Library for rules of use; OA articles are governed by the applicable Creative Commons License

Table 2. The 32 GLE Events[a]

GLE Events[b]		GLE Time[c]		GLE Peak					
No.	Date (DD.MM.YY)	T_{stc} (UT)	T_{pkc} (UT)	Increase Rate I_r (%)[d]	$T_{pkc} - T_{pkf}$[e] ΔT_1 (min)	$T_{pkc} - T_{cme}$[f] ΔT_2 (min)	$T_{cme} - T_{pkf}$[g] ΔT_3 (min)	$T_{str} - T_{pkc}$[h] ΔT_4 (min)	$T_{cme} - T_{endr}$[i] ΔT_5 (min)
33	21.08.79	0640	0645	4.21	+032			33	
34	10.04.81	1745	1800	2.64	+057			61	
35	10.05.81	0615	0625	3.58	+066			12	
37	26.11.82	0300	0620	4.55	+223			34	
* 38	07.12.82	2350	0015	25.74	+021			10	
* 39	16.02.84	0905	0910	14.96	+087			07	
40	25.07.89	0850	1110	2.97	+147			06	
* 41	16.08.89	0145	0300	12.44	+103			42	
* 42	29.09.89	1135	1350	173.80	+137			13	
* 43	19.10.89	1310	1515	37.89	+160			20	
* 44	22.10.89	1810	1845	16.61	+048			28	
* 45	24.10.89	1820	2020	94.42	+109			40	
46	15.11.89	0705	0710	5.16	+005			10	
* 47	21.05.90	2230	2250	12.93	+033			18	
* 48	24.05.90	2110	0130	10.9[j]	+281			22	
49	26.05.90	2055	2140	6.2	+042			07	
50	28.05.90	1000	1130	4.69	+202			82	
51	11.06.91	0230	0345	7.70	+076			28	
* 52	15.06.91	0840	0925	24	+054			115	
53	25.06.92	2035	2100	5.62	+049			41	
* 55	06.11.97	1155	1315	10.91	+080	+065	15	03	07
56	02.05.98	1355	1410	6.84	+033	+004	96	17	197
* 59	14.07.00	1030	1100	29.46	+036	+006	30	23	41
* 60	15.04.01	1400	1435	57.02	+045	+029	16	28	129
* 61	18.04.01	0225	0310	14.94	+056	+040	16	08	03
62	04.11.01	1635	1720	3.57	+060	+045	15	24	40
63	26.12.01	0550	0615	8.35	+035	+045	−10	49	160
64	24.08.02	0115	0135	6.45	+023	+008	15	07	08
65	28.10.03	1125	1150	7.37	+040	+020	20	80	66
67	02.11.03	1730	1755	8.00	+030	+025	05	16	54
* 69	20.01.05	0615	0700	269.57	+000	+006	−6	96	169
* 70	13.12.06	0235	0305	92.43	+025	+011	14	10	47

[a]Peak increase rates (I_r %) have been deduced based on the availability of 5-min pressure-corrected data of CRI from the Oulu neutron monitor (ONM). In ΔT_1(min), + indicates that peak time (T_{pkf}) of the solar flare is earlier than peak time of the GLE (T_{pkc}). Similarly, in ΔT_2 (min) + indicates that time of appearance of CME is earlier than the peak time of GLE. Thus, in ΔT_3(min) + indicates flare peak time is earlier than CME appearance time, and in ΔT_4(min) + indicates solar radio burst start time (T_{str}) is earlier than GLE peak time. In ΔT_5(min) + indicates that time (T_{cme}) of appearance of CME is earlier than the end time (T_{endr}) of radio burst type II. * Events marked with an asterisk (*) denote the important GLE events having an increase rate ≥10%.

[b]GLE event number (No.) and occurrence date.

[c]Start time (T_{stc}), and peak time (T_{pkc}).

[d]Increase rate (I_r %) of GLE.

[e]Time difference ($\Delta T_1 = T_{pkc} - T_{pkf}$) between peak time of GLE and X-ray flare (e.g., Figure 4).

[f]Time difference ($\Delta T_2 = T_{pkc} - T_{cme}$) between peak time of GLE and appearance time of CME.

[g]Time difference ($\Delta T_3 = T_{cme} - T_{pkf}$) between first appearance of CME and flare peak.

[h] Time difference ($\Delta T_4 = T_{str} - T_{pkc}$) between start time of solar radio type II burst and peak time of GLE.

[i]The time difference ($\Delta T_5 = T_{cme} - T_{endr}$) between CME and radio type II end time. Each time difference is computed within the time window of each GLE separately.

[j]GLE48 started at 2110 (UT) on 24.05.1990 when peak intensity was on 25.05.1990 at 0130 (UT).

associated with very high speed CMEs (Table 1). If CMEs are triggered from solar flares then the association of high-speed CMEs with strong flares is perhaps reasonable. The association between very fast CMEs and strong solar flares during GLE events indicates that the strong flare and very fast CME-driven shocks may cause GLEs. But the time delay between shock and flare did not show precisely that the more the delay, the more the GLE enhancement or vice versa (Table 2). So, the criteria for the characteristics of GLE-associated CMEs are yet to be clarified [e.g., *Gopalswamy et al.*, 2005].

3.3. Characteristics of GLE-Associated SEP

[24] Solar energetic particle fluxes are thought to be produced during large solar eruptions. SEP fluxes can also originate either from energetization at a solar flare site or by shock waves associated with CMEs. Our observations revealed that SEP fluxes are one of the main perpetrators causing GLE. Most of the GLE-associated SEP fluxes show that there are two parts to the patterns of fluxes, the softer part and the harder part, that may modulate cosmic rays differently. The harder part refers to the extreme intensity, while the softer part refers to the weak intensity [e.g., *Firoz and Kudela*, 2007]. The harder part of SEP fluxes seems to be causing GLEs. Although intense SEP fluxes can be observed extended a few minutes even after the GLE peak, the GLE peak is often integrated with the onset of the rising part of the SEP fluxes. The general patterns of non-GLE-associated SEP fluxes are very different from the patterns of GLE-associated SEP fluxes (Figures 6 and 7). The softer

21562202a, 2010, A9, Downloaded from https://agupubs.onlinelibrary.wiley.com/doi/10.1029/2009JA015023, Wiley Online Library on [13/06/2025]. See the Terms and Conditions (https://onlinelibrary.wiley.com/terms-and-conditions) on Wiley Online Library for rules of use; OA articles are governed by the applicable Creative Commons License

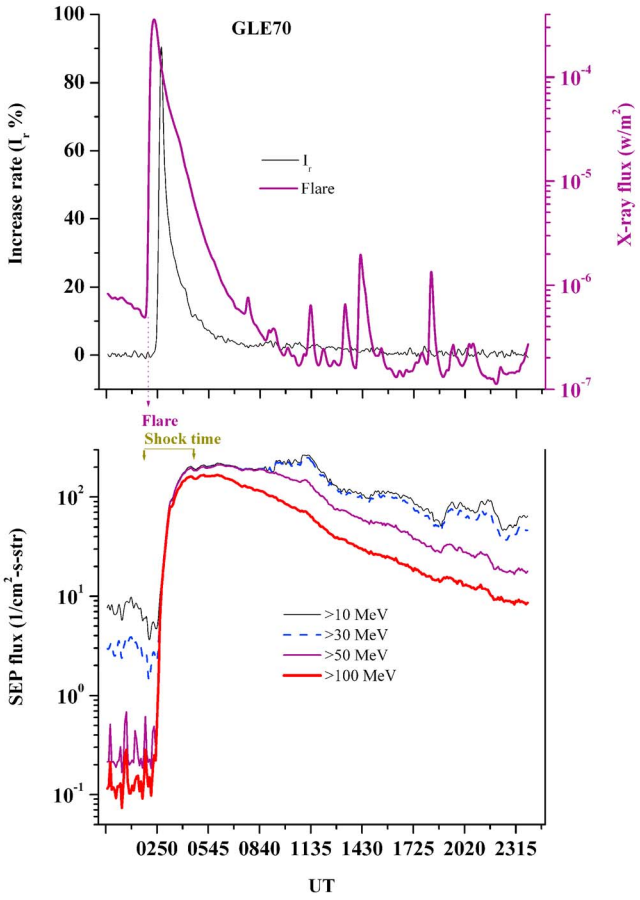

Figure 6. (top) GLE70 at ONM and the associated X-ray fluxes. (bottom) Simultaneous SEP fluxes of different energy channels. The conjunction between time of flare peak and time of shock is shown by the point arrow. In terms of type II solar radio burst, start time and end time of the shock waves within the time window of each GLE have been considered (Table 1). GLE, ground-level enhancements; ONM, Oulu Neutron Monitor; SEP, solar energetic particle.

and harder parts of non-GLE-associated SEP fluxes evolve abruptly. For instance, November 4, 2003 had a very fast (2657 km/s) halo CME at 1954 (UT) followed by a very strong (3B/X28.0) flare (1.8×10^{-3} w/m^2) at 1945 (UT), but it did not cause any sort of GLE event (Figure 7). In addition, we found that 2004 was a year of non-GLE events although the fastest halo CME speed (3387 km/s) on 10 November 2004 at 0226 (UT) followed by an X-class (0.2×10^{-3} w/m^2) flare at 0215 (UT) was available (figure not shown). This finding agrees with the earlier report of *Uddin et al.* [2006]. Thus, we are convinced that harder SEP fluxes may often cause GLEs.

[25] To check results of the investigations of non-GLE- and GLE-associated SEP fluxes, we further studied corresponding fluences of SEP fluxes. We found that most (~88%) of SEP fluences related to GLEs were very strong. There were only three relatively softer particle fluences, namely, 0.81×10^5 cm^{-2}, 0.82×10^6 cm^{-2}, and 0.71×10^6 cm^{-2} across GLE47, GLE48, and GLE53, respectively (Table 1). On an average, the fluence (1.61×10^6 cm^{-2}) of particle flux >10 MeV across non-GLE events was much softer than the fluence (0.45×10^8 cm^{-2}) of particle flux >10 MeV across GLE event (Figure 8). The strong fluences were associated with GLEs that were also associated with fast CMEs and intense flares (Table 1). Earlier, *Smart and Shea* [2002] also indicated that major solar particle fluence events are associated with solar flare and fast CME.

[26] Since the propagation speed of SEP flux depends on energy [*Kuwabara et al.*, 2006], the variability of SEP-associated GLE, subsequently, depends on the variability of SEP flux. Variability of the solar eruptions may be the main factor for the variability of SEPs with respect to solar locations and that the time of GLE can be affected by the solar location [*Bieber et al.*, 2005]. Therefore, the variability in the increase rate (%) of GLE may depend upon the magnitude of the solar energetic particle eruptions. There are presumably also some other reasons for GLE variations. For example, the chemical reaction of the particles is caused by various scattering effect presumably in middle atmosphere where atmosphere chemistry is known to be affected by cosmic rays [e.g., *Kane*, 2009]. Evidently, the daily averaged CRIs of GLE events (Figure 2) show a periodic pattern with an increment in the initial events followed by decrement in the center-scale and again the latter events with increment. This obeys the inverse proportionality with the solar cycle, which means that GLE variation depends not only on the potentiality of solar flare, CME, and SEP, but also on some other solar, interplanetary, and geophysical parameters. Longitudinal effects might also be responsible for the variation in GLE.

4. General Discussion

[27] We observed that most of the strong flares were associated with very fast CMEs (Table 1), but there might be a rare case in which those criteria are apparently inactive. For example, the C-class (C2.2) flare was associated with GLE61 when the CME speed (2465 km/s) was extremely fast in the sky plane. We consider that this GLE might be caused by the CME. However, as explained earlier, the high-speed CME association does not confirm the GLE production; rather the high-speed CME may drive shocks relatively faster that promote the enhancement in cosmic ray intensity. The mechanism is that GLE61 was associated apparently with a weaker flare, but actually the flare having greater optical importance (2B) was strong enough while existing behind the west limb at the location (S 20, W limb) of the solar disk (Table 1). We noticed that the flare during GLE61 was apparently not strong, because the angular extent through which the flare particles propagate was very small. The CME speed (2465 km/s) was very high because the CME was much extended. In fact, a CME that originated from the limb is likely to be much less affected by the projection effect. The CME trajectory from the west limb is much less deflected by the solar rotation. These arguments are in good agreement with previous investigators [*Moon et al.*, 2005; *Lin et al.*, 2006].

[28] As discussed earlier, GLE is associated with fast CME, but it is still difficult to confirm that the fast CME is the criterion to cause the GLE event because fast CME can be also found over non-GLE events. For instance, the

21562202a, 2010, A9, Downloaded from https://agupubs.onlinelibrary.wiley.com/doi/10.1029/2009JA015023, Wiley Online Library on [13/06/2025]. See the Terms and Conditions (https://onlinelibrary.wiley.com/terms-and-conditions) on Wiley Online Library for rules of use; OA articles are governed by the applicable Creative Commons License

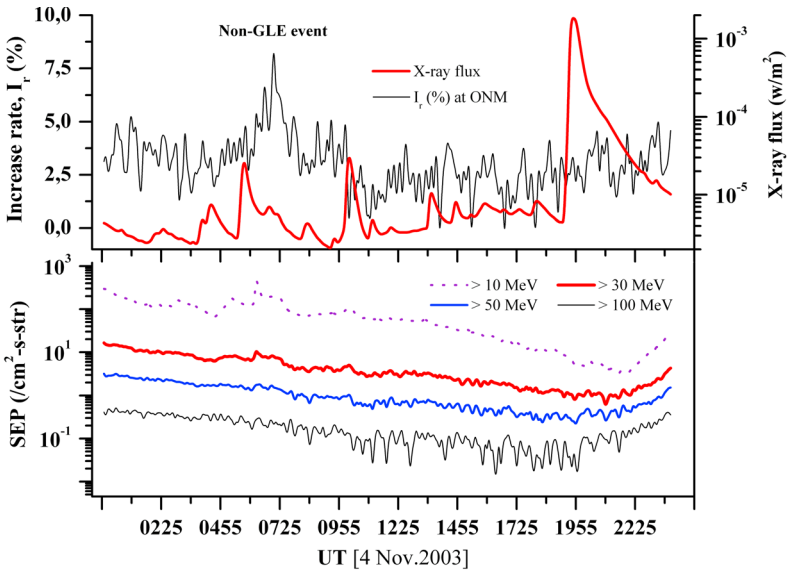

Figure 7. General patterns of GLE associated SEP fluxes and non-GLE-associated SEP fluxes are different. An example is shown here. (top) Increase rate (I_r %) of CRI and corresponding flare during non-GLE event on November 4, 2003. (bottom) The simultaneous SEP fluxes of different energy bands during the same non-GLE event. CRI, cosmic ray intensity; GLE, ground-level enhancements; SEP, solar energetic particle.

highest CME speed (3387 km/s) on November 10, 2004 at 0226 (UT) was observed across a non-GLE event. On the contrary, there was rare GLE events when CME speed was not fast enough. For example, the GLE69 associated with the lowest fast (882 km/s) Halo CME was a very strong GLE. We propose that the strong flare (X7.1) having better optical importance (3B) perhaps produced GLE69. The flare and shock time during GLE69 indicate that the flare and shock conjunction might be also responsible (Table 1).

[29] The characteristics of SEP fluxes during GLE events and non-GLE events indicate that harder SEP flux could be one of the sole perpetrators that often cause GLE. However, there is still no widely accepted theory that explains all the observed properties of SEPs [*Gopalswamy et al.*, 2004], and that rare event may be observed. For example, 12–20 November 1998 is a non-GLE event (figure not shown). Over this event, the SEP flux showed similar characteristics that are usually seen across GLE. Nevertheless, no GLE took place. Therefore, SEP flux is not the only perpetrator causing GLEs, there might be some other solar agents that sometimes also cause GLEs.

5. Summary

[30] In this paper, we explained how to deduce the increase rate of GLE, and accordingly deduced increase rates (%) of 32 GLEs. Then, we discussed characteristics of GLE-associated flares, CMEs, and SEP fluxes. We showed that intense solar energetic particles and sometimes powerful solar flares seem to be causing GLE. Our results can be summarized as follows.

[31] 1. Most (~82%) of the GLEs are associated with X-class flares. Almost all GLE-associated flares originated from the western hemisphere of the Sun. Most of the X-ray flares that were associated with GLE of increase rate >10% originated from the southwest active region. The rising portion of X-ray flare with strong optical signatures may sometimes generate GLE. Above all, when the GLE follows the flare X-ray flux without significant delay, then the flare seems to cause the GLE.

[32] 2. Most of the GLEs associated with strong flares were also associated with fast CMEs. On the average, the speed (1726.17 km/s) of GLE-associated CMEs was much faster than the speed (423.39 km/s) of non-GLE-associated CMEs. Although the fast Halo CME is usually associated with GLE, it alone does not seem to cause GLEs, because its first appearance is always across the descending phase or even in the background after the peak of GLE. CME causes geomagnetic turmoil that may modulate GLE.

[33] 3. Characteristics of SEP fluxes during GLE events and non-GLE events imply that the greatly increased SEP flux is necessary to cause GLE. The results are also supported by SEP fluences. Approximately 88% of fluences of SEP fluxes related to GLEs were stronger. On the average, the fluence (~1.61×10^6 cm^{-2}) of SEP flux >10 MeV across non-GLE events was much softer than the fluence (~0.45×10^8 cm^{-2}) of SEP flux >10 MeV across GLE events.

6. Conclusion

[34] Harder energetic particle fluxes having strong fluences are presumably necessary for causing GLEs. Since a solar flare is a violent explosion of solar energetic particles, it may also sometimes cause GLE. The solar flare characterized by direct proportionality with GLE peak seems to be responsible. Alternatively, a conjunction between CME-driven interplanetary shock and flare may produce GLE. CME alone presumably does not cause GLE. The variation of the GLEs may depend on the magnitude of the intensity of the flare, solar energetic particle, and CME-driven

21562202a, 2010, A9, Downloaded from https://agupubs.onlinelibrary.wiley.com/doi/10.1029/2009JA015023, Wiley Online Library on [13/06/2025]. See the Terms and Conditions (https://onlinelibrary.wiley.com/terms-and-conditions) on Wiley Online Library for rules of use; OA articles are governed by the applicable Creative Commons License

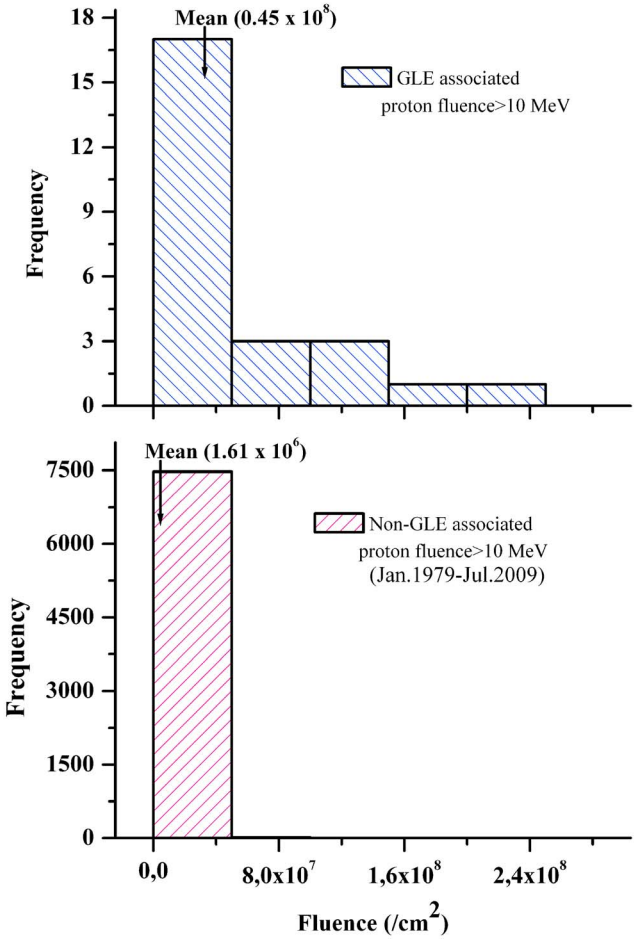

Figure 8. (top) Distributions of the fluences (per cm^2) of proton fluxes >10 MeV associated with GLE events and (bottom) the distributions of fluences (per cm^2) of proton fluxes >10 MeV associated with non-GLE events are shown for the period of January 1979 through July 2009.

interplanetary shock. Sometimes, other solar, interplanetary, and geophysical parameters may also be responsible for the variability.

[35] In a further study, an extended investigation into GLE-associated solar, interplanetary, and geophysical parameters, and longitudinal variations of GLEs will be conducted based on high-resolution data of cosmic ray intensity from different neutron monitor stations and space satellites.

[36] **Acknowledgments.** This work was supported by the "Development of Korean Space Weather Center" of KASI and the KASI basic research funds. Data from the NGDC, CDAW, and GOES space satellites and data of the neutron monitor at Oulu have been utilized. We thank the anonymous adjudicator for constructive comments and suggestions that developed the manuscript. We also thank the anonymous reviewers for their comments. Karel Kudela collaborated in this study through VEGA grant agency project 2/0081/10.

[37] Philippa Browning thanks Rajaram Kane, Stephan C. Buchert and other reviewers for their assistance in evaluating this paper.

References

Andrews, M. D. (2003), A search for CMEs associated with big flares, *Sol. Phys.*, *218*, 261–279.

Belov, A. V. (2009), Properties of solar X-ray flares and proton event forecasting, *Adv. Space Res.*, *43*, 467–473.

Belov, A. V., E. A. Eroshenko, H. Mavromichalaki, C. Plainaki, and V. Yanke (2005), Solar cosmic rays during the extremely high ground level enhancement on 23 February1956, *Ann. Geophys.*, *23*, 2281–2291.

Bieber, J. W., J. Clem, P. Evenson, and R. Pyle (2005), Relativistic solar neutrons and protons on 28 October 2003, *Geophys. Res. Lett.*, *32*, L03S02, doi:10.1029/2004GL021492.

Braun, I., et al. (2005), Solar modulation of cosmic rays in the range from 10 to 20 GeV, *Conf. Pap. Int. Cosmic Ray Conf. XXIX*, *2*, 135–138.

Cliver, E. W. (2006), The unusual relativistic solar proton events of 1979 August 21 and 1981 May 10, *Astrophys. J.*, *639*, 1206–1217.

Cliver, E. W., S. W. Kahler, M. A. Shea, and D. F. Smart (1982), Injection onsets of ~2 GeV protons, ~1 MeV electrons and ~100 keV electrons in solar cosmic ray flares, *Astrophys. J.*, *260*, 362–370.

Cliver, E. W., S. W. Kahler, and D. V. Reames (2004), Coronal shocks and solar energetic proton events, *Astrophys. J.*, *605*, 902–910.

Dennis, B. R., and D. M. Zarro (1993), The Neupert effect: What can it tell us about the impulsive and gradual phases of solar flares?, *Sol. Phys.*, *146*, 177–190.

Dorman, L. I. (2004), *Cosmic Rays in the Earth's Atmosphere and Underground*, Kluwer Acad., Dordrecht, Netherlands.

Dorman, L. I., and L. A. Pustil'nik (2005), On the probability of solar cosmic ray fluency during SEP event in dependence of the level of solar activity, *Conf. Paper Int. Cosmic Ray Conf. XXIX*, *2*, 331–334.

Dorman, L. I., and D. Venkatesan (1993), Solar cosmic rays, *Space Sci. Rev.*, *64*, 183–362.

Duldig, M. L. (1994), Cosmic ray transient variations observed from the Earth, *Publ. Astron. Soc. Aust.*, *11*(2), 110–115.

Duldig, M. L. (2001), Australian cosmic ray modulation research, *Publ. Astron. Soc. Aust.*, *18*, 12–40.

El-Borie, M. A. (2003), Major solar-energetic particle fluxes: I. Comparison with the associated ground level enhancements of cosmic rays, *Astroparticle Phys.*, *19*(4), 549–558.

Firoz, K. A. (2008), On cosmic ray diurnal variations: Disturbed and quiet days, in *WDS'08 Proceedings of Contributed Papers*, part II: *Physics of Plasmas and Ionized Media*, edited by J. Safrankova and J. Pavlu, pp. 183–188, Matfyzpress, Prague.

Firoz, K. A., and K. Kudela (2007), Cosmic rays and low energy particle fluxes, in *WDS'07 Proceedings of Contributed Papers*, part II: *Physics of Plasmas and Ionized Media*, edited by J. Safrankova and J. Pavlu, pp. 106–110, Matfyzpress, Prague.

Firoz, K. A., D. V. Phani Kumar, and K.-S. Cho (2009), On the relationship of cosmic ray intensity with solar, interplanetary and geophysical parameters, *Astrophys. Space Sci.*, *325*(2), 185–193, doi:10.1007/s10509-009-0181-9.

Flückiger, E. O., R. Bütikofer, L. Desorgher, and M. R. Moser (2006), The role of GLEs in space weather, paper presented at 36th COSPAR Scientific Assembly, Beijing, China.

Gaisser, T. K. (1990), *Cosmic Rays and Particle Physics*, Cambridge Univ. Press, Cambridge, U. K.

Gopalswamy, N., S. Yashiro, S. Krucker, G. Stenborg, and R. A. Howard (2004), Intensity variation of large solar energetic particle events associated with coronal mass ejections, *J. Geophys. Res.*, *109*, A12105, doi:10.1029/2004JA010602.

Gopalswamy, N., H. Xie, S. Yashiro, and I. Usoskin (2005), Coronal mass ejections and ground level enhancements, paper presented at 29th International Conference on Cosmic Rays, Tata Inst. of Fundam. Res., Pune, India.

Harrison, R. A. (1995), The nature of solar-flares associated with coronal mass ejection, *Astron. Astrophys. J.*, *304*, 585–594.

Hillas, Y. A. M. (1972), *Cosmic Rays*, Pergamon Press, Oxford, U. K.

Jing, J., J. Qiu, J. Lin, M. Qu, Y. Xu, and H. Wang (2005), Magnetic reconnection rate and flux-rope acceleration of two-ribbon flares, *Astrophys. J.*, *620*, 1085–1091.

Kahler, S. W., E. Hildner, and M. A. I. van Hollebeke (1978), Prompt solar proton events and coronal mass ejections, *Sol. Phys.*, *57*, 429–443.

Kahler, S., D. Reames, and N. Sheeley Jr. (2001), A CME associated with an impulsive SEP event, *Conf. Paper Int. Cosmic Ray Conf. XXVII.*, 3443–3448.

Kane, R. P. (2009), High amplitude anisotropic events (HAE) in cosmic ray diurnal variation during solar cycle 23, *Ind. J. Radio Space Phys.*, *38*, 189–196.

Kudela, K., M. A. Shea, D. F. Smart, and L. C. Gentile (1993), Relativistic solar particle events recorded by the Lomnicky Stit Neutron Monitor, *Conf. Paper Int. Cosmic Ray Conf.*, *3*, 71.

Kudela, K., M. A. Shea, D. F. Smart, L. C. Gentile (1993), Relativistic solar proton events recorded by the Lomnicky Stit neutron monitor, paper

21562202a, 2010, A9, Downloaded from https://agupubs.onlinelibrary.wiley.com/doi/10.1029/2009JA015023, Wiley Online Library on [13/06/2025]. See the Terms and Conditions (https://onlinelibrary.wiley.com/terms-and-conditions) on Wiley Online Library for rules of use; OA articles are governed by the applicable Creative Commons License

presented at 23rd International Cosmic Ray Conference, Int. Union of Pure and Appl. Phys., Calgary, Alberta, Canada.
Kurt, V., A. Belov, H. Mavromichalaki, and M. Gerontidou (2004), Statistical analysis of solar proton events, *Ann. Geophys.*, *22*, 2255–2271.
Kuwabara, T., et al. (2006), Real-time cosmic ray monitoring system for space weather, *Space Weather*, *4*, S08001, doi:10.1029/2005SW000204.
Lin, R. P., et al. (2006), Particle acceleration by the sun: Electrons, hard x-rays/gamma-rays, *Space Sci. Rev.*, *124*, 233–248.
Longair, M. S. (1992), Particles, photons and their detection, in *High Energy Astrophysics*, vol. 1, 2nd ed., Cambridge Univ. Press, Cambridge, U. K.
Manchester, W. B., et al. (2005), Coronal mass ejection shock and sheath structures relevant to particle acceleration, *Astrophys. J.*, *622*, 1225–1239.
Mavromichalaki, H., et al. (2007), GLEs as a warning tool for radiation effects on electronics and systems, a new alert system based on real-time neutron monitors, *IEEE Trans. Nuclear Sci.*, *54*(4), 1082–1088.
Meyer, P., E. N. Parker, and J. A. Simpson (1956), Solar cosmic rays of February 1956 and their propagation through interplanetary space, *Phys. Rev.*, *104*, 768–783.
Miroshnichenko, L. I. (2001), *Solar Cosmic Rays*, Kluwer Acad., Dordrecht, Netherlands.
Moon, Y.-J., K.-S. Cho, M. Dryer, Y.-H. Kim, S.-C. Bong, J. Chae, and Y. D. Park (2005), New geoeffective parameters of very fast halo coronal mass ejections, *Astrophys. J.*, *624*, 414–419.
Park, P. N. (1957), Acceleration of cosmic rays in solar flares, *Phys. Rev.*, *107*, 830–836.
Reames, D. V. (1995), Solar energetic particles: A paradigm shift, *U.S. Natl. Rep. Int. Union Geod. Geophys. 1991-1994*, *Rev. Geophys.*, *33*, 585–591.
Reames, D. V. (1997), Energetic particles and the structure of coronal mass ejections, *Coronal Mass Ejections*, *Geophys. Monogr. Ser.*, vol. 99, edited by N. Crooker, J. A. Jocelyn and J. Feynman, pp. 217–222, AGU, Washington, D. C.
Shanmugaraju, A., Y.-J. Moon, K.-S. Cho, N. Gopalswamy, and U. Umapathy (2008), Investigation of CME dynamics in the LASCO field of view, *Astron. Astrophys.*, *484*, 511–516.
Shea, M. A., D. F. Smart and G. A. M. Dreschhoff (1999), Identification of major proton fluence events from nitrates in polar ice cores, *Radiat. Measure.*, 309–316.
Smart, D. F., and M. A. Shea (2002), Comment on estimating the solar proton environment that may affect Mars missions, *Adv. Space Res.*, *31*, 45–50.
Smart, D. F., M. A. Shea, and K. G. McCracken (2006), The Carrington event possible solar proton intensity-time profile, *Adv. Space Res.*, *38*, 215–225.
Uddin, W., R. Chandra, and S. S. Ali (2006), Extremely energetic 4B/X17.2 flare and associated phenomena, *J. Astrophys. Astron.*, *27*(2–3), 267–276.
Vršnak, B., D. Ruždjak, D. Sudar, and N. Gopalswamy (2004), Kinematics of coronal mass ejections between 2 and 30 solar radii: What can be learned about forces governing the eruption?, *AstroN. Astrophys.*, *423*, 717–728.
Wang, R., and J. Wang (2006), Investigation of the cosmic ray ground level enhancements during solar cycle 23, *Adv. Space Res.*, *38*, 489–492.
Yashiro, S., G. Michalek, S. Akiyama, N. Gopalswamy, and R. A. Howard (2008), Spatial relationship between solar flares and coronal mass ejections, *Astrophys. J.*, *673*, 1174–1180.

K.-S. Cho, K. A. Firoz, J. Hwang, J. J. Lee, and D. V. Phani Kumar, Solar and Space Weather Research Group, Korea Astronomy and Space Science Institute, Daejeon 305–348, South Korea. (kafiroz@kasi.re.kr; kazifiroz2002@gmail.com)

L. I. Dorman, Israel Cosmic Ray and Space Weather Center and Emilio Segre' Observatory, Technion and Israel Space Agency, Qazrin 12900, Israel.

S. C. Kaushik, School of Studies in Physics, Jiwaji University, Gwalior, M.P. 474001, India.

K. Kudela and M. Rybanský, Institute of Experimental Physics, Slovak Academy of Sciences, 04001 Košice, Slovakia.

S. Y. Oh, Bartol Research Institute, University of Delaware, Newark, DE 19716, USA.

21562202a, 2010, A9, Downloaded from https://agupubs.onlinelibrary.wiley.com/doi/10.1029/2009JA015023, Wiley Online Library on [13/06/2025]. See the Terms and Conditions (https://onlinelibrary.wiley.com/terms-and-conditions) on Wiley Online Library for rules of use; OA articles are governed by the applicable Creative Commons License